Manganese Complexes as Drying Catalysts for Alkyd Paints

Gorkum, R. van

6

A non-paint topic:

trigonal prismatic vs octahedral coordination geometry for the Mn(II) complexes $[Mn(acac)_2(bpy)]$ and $[Mn(acac)_2(phen)]$.†

Abstract

In this chapter is presented the first example of a mixed-ligand Mn(II) complex having a trigonal prismatic coordination geometry with simple, innocent, didentate ligands. The solution and solid state structures of $[Mn(acac)_2(bpy)]$, as studied by EPR spectroscopy, magnetic susceptibility measurements and XRD are presented: single crystals are hexagonal, space group $P6_1$ with unit cell dimensions a = 8.0482(9) Å, c = 51.602(10) Å, V = 2894.6(7) Å^3 and Z = 6. The complex has the trigonal prismatic geometry only in the solid state. Density functional theory (DFT) calculations were performed to address the question of the preference for a specific coordination geometry in the related Mn(II) complexes $[Mn(acac)_2(bpy)]$ (trigonal prismatic) and $[Mn(acac)_2(phen)]$ (distorted octahedral). Based on the very small energy differences for the calculated trigonal prismatic and octahedral structures it has been concluded that crystal packing effects must contribute largely in determining the trigonal prismatic structure for $[Mn(acac)_2(bpy)]$.

†This chapter is based on: R. van Gorkum, F. Buda, H. Kooijman, A. L. Spek, E. Bouwman and J. Reedijk, *Eur. J. Inorg. Chem.* submitted for publication.

6.1 Introduction

Even though the first observed example of a trigonal prismatic complex, [Re(1,2-$S_2C_2Ph_2)_3$], dates back from 1965,[1] mixed-ligand trigonal prismatic complexes with simple didentate ligands are still rare. Since 1965 several tris(dithiolene) complexes with trigonal prismatic or distorted octahedral geometry have been reported.[2] In addition a limited, but growing number of examples of non-dithiolene [M(didentate)$_3$] trigonal prismatic compounds is known, for instance with buta-1,3-diene, methylvinylketone or acetylacetonate as ligands.[3-6] A few mixed ligand trigonal prismatic complexes of the form [M(didentate1)$_2$(didentate2)] are known, for example the complexes with a diimine and two (substituted) catechol semiquinonates as ligands, [7-9] but they are definitely not as common as homoleptic tris(didentate) complexes. Most compounds mentioned above have either non-innocent ligands, or ligands that can easily participate in π-(back) bonding. Therefore it is not unexpected that for these complexes the majority of arguments for favoring trigonal prismatic over octahedral geometry are electronic in nature, as for example: the overall charge of the complex, ligand field stabilization energy, matching of ligand and metal orbital energies, bonding between the ligand donor-atoms and π-bonding.[10, 11] Even some examples of six-coordinated trigonal prismatic complexes with monodentate ligands have been reported.[12, 13] These complexes all contain d^0 metal ions and in these cases the preference for the trigonal prismatic geometry has been ascribed to the absence of steric or π-bonding effects.

A well-known strategy for obtaining trigonal prismatic complexes is using rigid, penta- or hexadentate ligands that force the trigonal prismatic geometry upon a complex by means of steric constraints.[14-16] This successful strategy has resulted in many examples of trigonal prismatic complexes.

While searching for novel manganese-based catalysts for the oxidative drying of alkyd paints (see the previous chapters),[17] the X-ray structure of the well-known compound [Mn(acac)$_2$(bpy)] was determined. Although this complex has been claimed to have an octahedral coordination geometry,[18] it appears to be the first example of a mixed-ligand complex with innocent didentate ligands that possesses the trigonal prismatic coordination geometry. Herein, the crystal structure details and EPR spectra of the complex are described. DFT calculations have been performed to address the question of the preference for trigonal prismatic versus octahedral geometry, comparing this complex with the related octahedral phenantroline complex [Mn(acac)$_2$(phen)].

6.2 Results

6.2.1 Synthesis and characterization

Both [Mn(acac)$_2$(bpy)] and [Mn(acac)$_2$(phen)] have been prepared by the same method, using a slight variation on a literature procedure. The synthesis of [Mn(acac)$_2$(bpy)] is best carried out under argon until the product is isolated and dried, since the complex is very sensitive to air-oxidation when moist or in solution. The dried complex is stable in air. The yield (67%) was satisfactory, as was the elemental analysis.

6.2.2 Spectroscopic features

The Infrared spectrum of $[Mn(acac)_2(bpy)]$ is in agreement with literature,[18] with important IR peaks being ν(C-O) 1604, 1578 cm^{-1}, ν(C-C) 1516 cm^{-1}, ν(M-O) 647, 536, 415 cm^{-1} and ν(M-N) 403, 228 cm^{-1}. The electronic spectrum of the solid compound shows an MLCT band at 365 nm (27.4×10^3 cm^{-1}).

6.2.3 EPR

The room temperature powder EPR spectrum of $[Mn(acac)_2(bpy)]$ shows a strong, non-isotropic resonance signal at g = 3.25 and a very weak signal at high field, at g = 0.74, see Figure 6.1. The powder spectrum of $[Mn(acac)_2(phen)]$ shows a single broad signal at g = 2 (see the inset in Figure 6.1).[19]

The frozen solution spectra (77 K, 1 mM in CH_2Cl_2/Toluene 1/1 v/v) of $[Mn(acac)_2(bpy)]$ and $[Mn(acac)_2(phen)]$ are nearly identical, showing a broad peak at g = 2.7 and a very broad signal (260-410 mT) centered around g = 2. The frozen solution spectrum of $[Mn(acac)_2(bpy)]$ is depicted in Figure 6.2. Overlapping the signal at g = 2 a six-line signal typical for octahedral manganese(II) is present, showing ^{55}Mn hyperfine structure and additional lines due to zero-field splitting. The average coupling constant due to the manganese hyperfine coupling is 97 G.

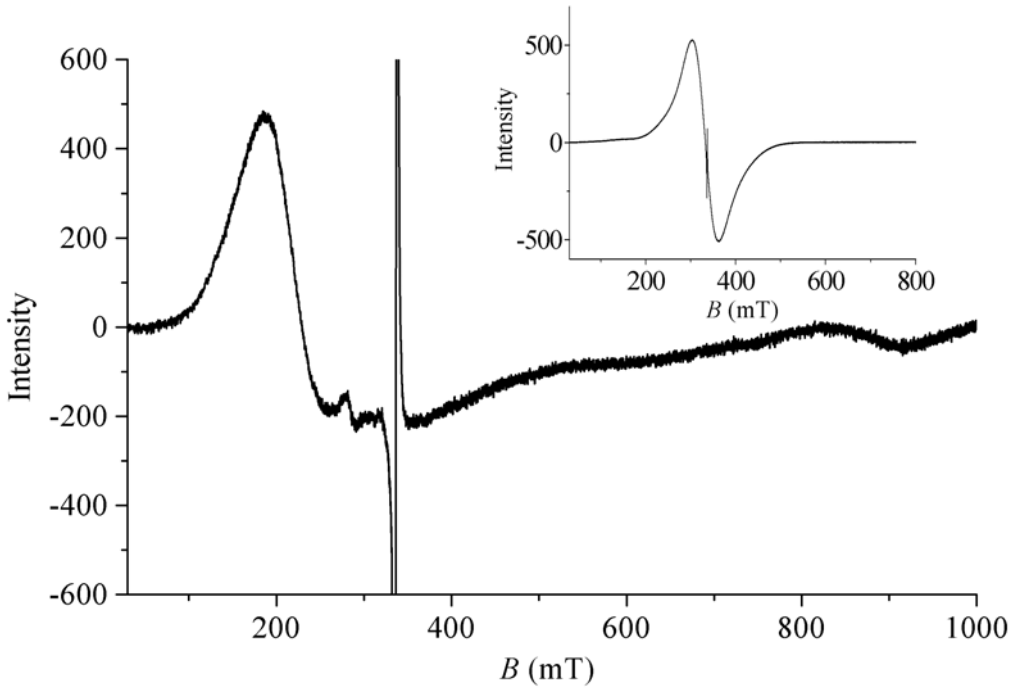

Figure 6.1: Room temperature powder EPR spectra of $[Mn(acac)_2(bpy)]$ and $[Mn(acac)_2(phen)]$ (inset). Important EPR parameters for both spectra: Freq = 9.434 GHz, power 4 mW. The dpph reference can be seen as a sharp radical signal at 336 mT. The small signal at 280 mT is due to an impurity in the cavity.

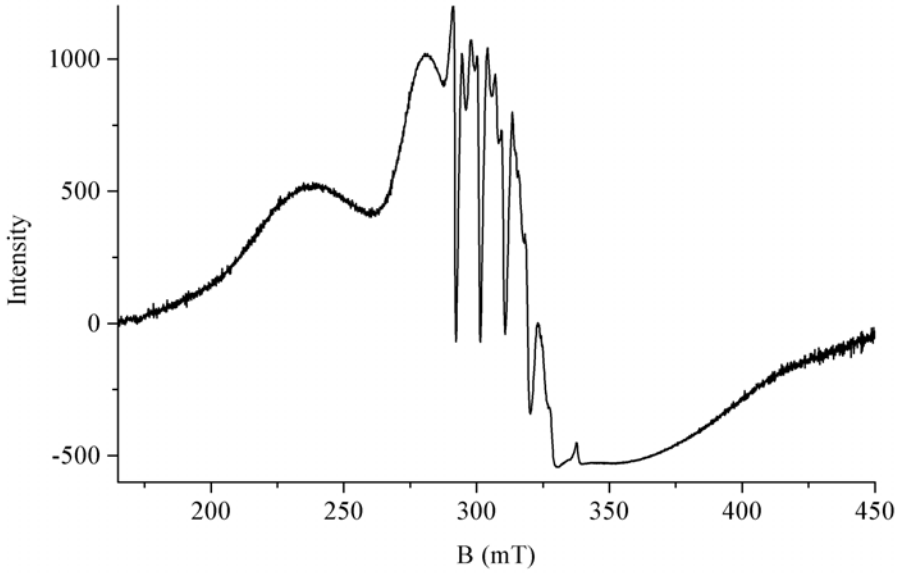

Figure 6.2: Frozen solution (77 K, 1 mM in CH_2Cl_2/toluene 1/1 v/v) X-band EPR spectra of $[Mn(acac)_2(bpy)]$. EPR parameters: Freq = 9.116 Ghz, power = 4 mW.

6.2.4 Magnetic Susceptibility

A χT vs T plot for $[Mn(acac)_2(bpy)]$ shows a straight line which declines at low temperatures, most likely due to the zero-field splitting of the Mn(II) ion.[20] Plotting χ^{-1} vs T also results in a straight line and thus the compound obeys the Curie-Weiss law. Fitting the data, the Curie and Weiss constants are obtained, being C = 4.137 $cm^{-3}Kmol^{-1}$ and θ = –1.35 K, respectively. The Curie constant allows for calculating the total molecular spin of the compound, and a value of S = 2.42 (≈5/2) is obtained. For $[Mn(acac)_2(phen)]$ a value of μ_{eff} = 6.2 μ_b is given in the literature, which also confirms an S = 5/2 spin state.[21]

6.2.5 Description of the crystal and molecular structure

Single crystals of $[Mn(acac)_2(bpy)]$ where obtained by letting the filtered reaction mixture stand overnight at –20 °C. The geometry of the complex and the atom-labeling scheme are shown in Figure 6.3. Selected bond lengths and angles are collected in Table 6.1.

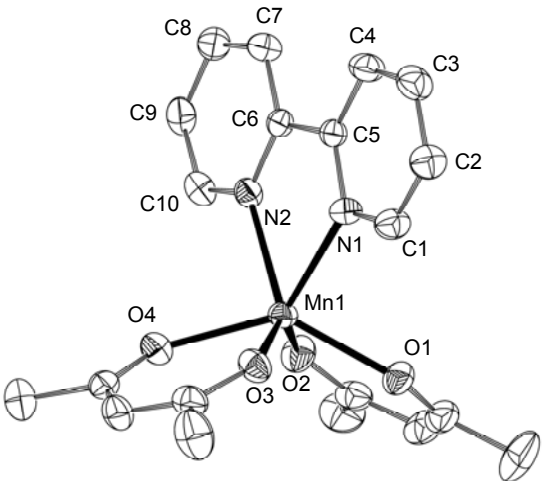

Figure 6.3: Ortep plot of $[Mn(acac)_2(bpy)]$, ellipsoids are shown at 50% probability. Hydrogen atoms are omitted for clarity

Table 6.1: Selected bond lengths (Å) and angles (°) experimentally obtained with XRD compared to values obtained by DFT calculations.

	prism			**octahedron**		
	X-ray	calculated		X-ray	calculated	
L	bpy	bpy	phen	phen	bpy	phen
Mn1-O1	2.1480(16)	2.1380	2.1373	2.116(5)	2.1235	2.1259
Mn1-O2	2.1580(18)	2.1314	2.1281	2.152(5)	2.1358	2.1231
Mn1-O3	2.1534(16)	2.1316	2.1290	2.152(5)	2.1321	2.1275
Mn1-O4	2.1572(17)	2.1382	2.1361	2.116(5)	2.1182	2.1229
Mn1-N1	2.288(3)	2.3395	2.3603	2.307(5)	2.3549	2.3488
Mn1-N2	2.283(2)	2.3382	2.3603	2.307(5)	2.3713	2.3491
O1-Mn1-O2	81.69(6)	82.81	82.99	84.0(2)	84.34	84.88
O3-Mn1-O4	81.92(6)	82.79	83.01	84.0(2)	84.65	84.89
N1-Mn1-N2	70.41(8)	68.61	69.53	72.6(2)	68.80	70.60
N1-Mn1-O1	85.12(7)	83.88	82.77	93.4(2)	90.70	89.02
N1-Mn1-O2	129.76(8)	125.57	123.32	90.8(2)	94.13	95.37
N1-Mn1-O3	85.99(7)	83.98	83.55	86.6(2)	86.36	86.82
N1-Mn1-O4	134.44(7)	133.73	134.91	163.0(2)	156.55	156.71
N2-Mn1-O1	132.45(7)	133.71	134.89	163.0(2)	156.20	157.20
N2-Mn1-O2	83.83(8)	84.11	83.55	86.6(2)	85.21	86.92
N2-Mn1-O3	131.01(7)	125.40	123.35	90.8(2)	96.82	96.14
N2-Mn1-O4	85.20(7)	83.90	82.79	93.4(2)	90.82	88.68
O1-Mn1-O3	84.83(6)	85.54	86.20	98.1(2)	93.68	92.71
O1-Mn1-O4	136.62(7)	138.54	138.64	102.0(2)	111.44	113.07
O2-Mn1-O4	82.52(6)	85.41	86.22	98.1(2)	95.63	93.97
O2-Mn1-O3	139.97(8)	146.46	149.13	176.7(2)	177.95	176.71
Torsion angles:						
N1-C5-C6-N2	3.0(3)	4.42	0.61	3.09	4.32	0.23
Ct1[a]-N2-N1-Ct2[b]	–2.1(3)	–5.92	–8.49	39.45	35.98	37.38
Ct1-O2-O1-Ct2	–1.9(3)	–5.44	–7.47	42.34	37.92	37.30
Ct1-O4-O3-Ct2	–2.5(3)	–5.54	–7.48	42.34	36.98	36.21

[a] Ct1 = Centroid of the triangular face O2-O4-N2, [b] Ct2 = centroid of triangular face O1-O3-N1

The manganese(II) ion has an almost perfect N_2O_4 trigonal-prismatic coordination environment, with two acetylacetonate ligands and one bipyridine ligand. The manganese to nitrogen distances are 2.288(3) and 2.283(2) Å. The manganese to oxygen distance for the acetylacetonate ligands is for each Mn-O bond almost the same, and lie in the range 2.1480(16) – 2.1580(18) Å. The bite angles for each of the acetylacetonate ligands are also nearly identical, being 81.69(6)° (O1-Mn1-O2) and 81.92(6)° (O3-Mn1-O4). Since the bite angles are rather small and the Mn-O distance rather large, the Mn-O-C angles are also large, in the range 130.39(17) – 131.78(16)°. The bipyridine ligand has a bite angle (N1-Mn1-N2) of 70.41°. The two acetylacetonate ligands are nearly planar, but the angle between the least-squares planes through the rings of the bipyridine ligand amounts to 3.79(12)°, and this ligand is thus not planar. For all three ligands, the atoms comprising the chelate rings deviate little from their least squares mean plane. The obtuse angles between the least-squares mean planes of the chelate rings lie in the range 117.67(7) – 121.30(6)°, in accordance with the trigonal prismatic coordination geometry.

The two trigonal faces of the prism constitute one oxygen atom of each of the acetylacetonate ligands and one nitrogen atom, thus forming O1-O3-N1 and O2-O4-N2. Figure 6.4 shows the trigonal prismatic coordination geometry around manganese in more detail, and the dimensions and angles of the prism are tabulated in Table 6.2. The lengths

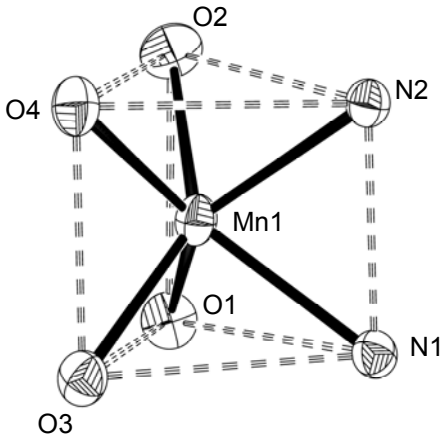

Figure 6.4: Trigonal prismatic geometry of $[Mn(acac)_2(bpy)]$ in detail

Table 6.2: Trigonal prism distances (Å) and angles (°) of $[Mn(acac)_2(L)]$, L = bpy (XRD & DFT data) or phen (only DFT)

	X-ray	**calculated**	
	bpy	bpy	phen
O1-N1	3.002(3)	2.996	2.978
O1-O3	2.901(2)	2.899	2.915
O3-N1	3.030(3)	2.995	2.996
O2-N2	2.968(3)	2.998	2.978
O2-O4	2.846(2)	2.896	2.914
O4-N2	3.007(3)	2.996	2.978
N1-N2	2.635(3)	2.636	2.692
O1-O2	2.816(2)	2.824	2.826
O3-O4	2.826(2)	2.823	2.827
O3-O1-N1	61.74(6)	57.88	61.10
O3-O1-O2	90.22(6)	90.99	91.24
O2-O1-N1	87.51(8)	86.16	85.79
O1-O2-N2	88.99(8)	89.86	91.02
O4-O2-N2	62.25(7)	61.08	60.50
O4-O2-O1	89.91(6)	88.73	88.28
O1-O3-N1	60.76(6)	61.08	60.49
O1-O3-O4	88.61(6)	88.66	88.25
O4-O3-N1	88.77(7)	90.06	90.98
O2-O4-O3	91.17(6)	91.17	91.25
O2-O4-N2	60.88(7)	61.14	61.10
O3-O4-N2	87.56(7)	86.05	85.82
O1-N1-O3	57.50(6)	57.88	58.41
N2-N1-O3	90.63(9)	89.50	87.90
N2-N1-O1	91.78(10)	93.70	94.10
O2-N2-O4	56.88(7)	57.78	58.40
O2-N2-N1	91.65(9)	89.57	87.88
O4-N2-N1	92.93(9)	93.75	94.08

of the triangular sides are in the range 2.901(2) – 3.030(3) Å for the triangle O1-O3-N1 and 2.846(2) – 3.007(3) Å for the triangle O2-O4-N2, all angles are in the range 56.88(7) – 62.25(7)°. The four acetylacetonate oxygens make up an almost exact square, the sides of which are in the range 2.816(2) – 2.901(2) Å. The remaining two faces of the prism are trapezoids consisting of two oxygen atoms of one acetylacetonate ligand and are joined by the two nitrogen atoms of bipyridine. Both faces have an O-O distance of 2.826(2) and 2.816(2) Å, an N-O distance in the range 2.968(3) – 3.030(3) Å and a markedly shorter distance of 2.635(3) Å for the N1-N2 side. Since the N1-N2 side is shorter than the O-O sides of the trapezoid faces of the prism, the two triangular faces are not parallel. The planes defined by O1-N1-O3 and O2-N2-O4 make an angle of 4.04(10)°. The torsion angles about the centroids of the triangular faces and each of the corners (for example Ct1-N1-N2-Ct2) are –2.1(3)°, –1.9(3)° and –2.5(3)°. A perfect trigonal prism would have angles of 0°, the triangular faces exactly overlapping.

The crystal structure has a hexagonal unit cell and space group $P6_1$. Figures 6.5, 6.6 and 6.7 show the packing in the *a*, *b* and *c* directions. The structure is composed of

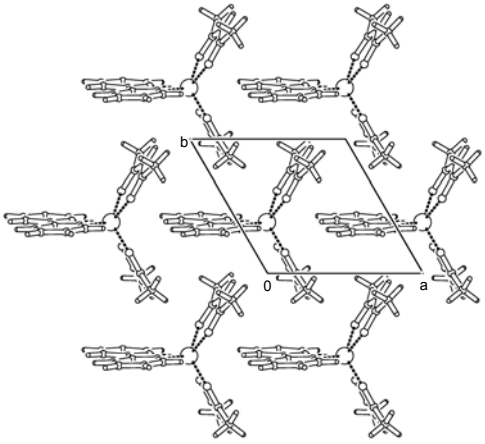

Figure 6.5: Crystal packing of $[Mn(acac)_2(bpy)]$ in the *a*-*b* plane. The acac methyl groups are packed together in rows along *a*.

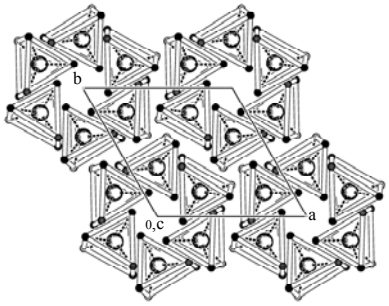

Figure 6.6: Projection of the crystal lattice of $[Mn(acac)_2(bpy)]$ down the c-axis. The lattice is composed of right-handed helices in the *c*-direction. Each complex in the helix is part of a layer in the *a*-*b* plane. Only the trigonal-prismatic polyhedra are shown for clarity.

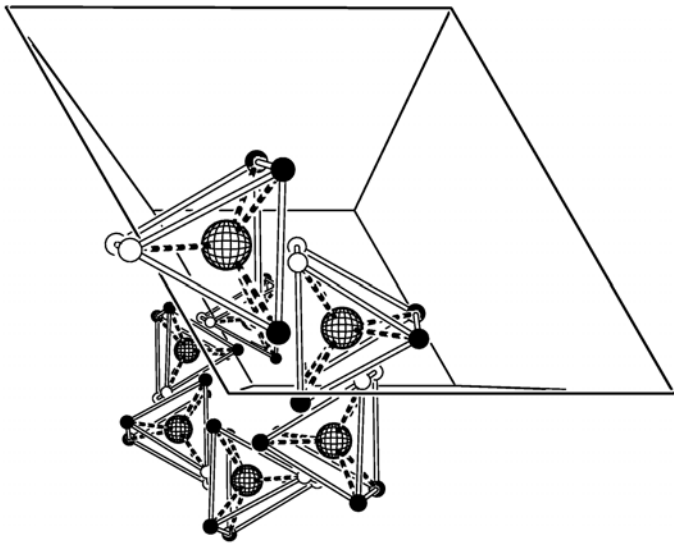

Figure 6.7: A perspective drawing of the crystal structure unit cell, clearly showing one of the helices along the *c*-axis. Only the trigonal-prismatic polyhedra are shown for clarity.

right-handed helices along the c-axis and therefore is chiral. A single helix consists of six molecules of [Mn(acac)$_2$(bpy)] per unit cell, due to the inherent hexagonal symmetry. The helices are tightly packed together in such a way that each molecule in the helix is part of a layer that extends in the a and b direction. Within such a layer, one can observe rows of [Mn(acac)$_2$(bpy)] molecules with aligned bipyridine ligands, each bipyridine pointing in-between the acetylacetonate ligands of the following molecule in the row. Due to this orientation, all acetylacetonate methyl groups are also packed together in rows.

6.2.6 DFT calculations

The DFT-B3LYP geometry optimization shows that the complex [Mn(acac)$_2$(bpy)] is stable in the trigonal prismatic structure in vacuum and that the high-spin (S=5/2) electronic state is the lowest energy configuration. Some of the theoretically predicted bond lengths and angles for this complex (in the vacuum) are reported in Table 6.2. The comparison between computed and experimental data in the crystal structure shows a good agreement. In particular the theory predicts that the bipyridine ligand is not planar, showing a small torsion angle of about 4° between its pyridine rings. The high-spin electronic configuration (S=5/2) is important for the stability of the trigonal prismatic geometry. Indeed, the optimized structure for S=3/2 is found to be about 34 kcal/mol higher in energy than the S=5/2 spin state. In the low-spin state S=1/2, the trigonal prismatic geometry is unstable and during the optimization the complex changes spontaneously towards an octahedral geometry.

To study the relative stability we have also optimized the complex [Mn(acac)$_2$(bpy)] in an octahedral coordination geometry in the vacuum. To obtain a relevant starting configuration the X-ray coordinates of the known octahedral compound [Mn(acac)$_2$(phen)] have been used,[22] removing C_{11} and C_{12} from the phen ligand in the coordinate file, thereby generating a bpy ligand. The final octahedral structure has an energy which is only a few tenths of a kcal/mol different from the energy of the trigonal-prismatic geometry. Given the typical accuracy of these calculations, the two structures can be considered energetically equivalent. The high-spin state is the lowest in energy also for the octahedral coordination geometry.

Subsequently the relative energy difference for the similar compound [Mn(acac)$_2$(phen)] was computed in a distorted octahedral environment and in a trigonal prismatic geometry for comparison. It turned out that for this compound the octahedral geometry is favoured by 1.5 kcal/mol over the trigonal prismatic one, both again favoring the S = 5/2 spin state.

6.3 Discussion

6.3.1 Structural features

The manganese to bipyridine distances 2.288(3) and 2.283(2) Å are not extraordinary and comparable to the Mn-N distances reported for the similar compound [Mn(acac)$_2$(phen)], which are 2.307 Å.[22] The bipyridine ligand has a bite angle (= N1-Mn1-N2) of 70.41°, which is quite small and can be related to the large ionic radius of Mn(II). Unsubstituted bipyridine ligands in manganese complexes commonly have bite angles varying between 72°-80°.[23] Simple donor-atom to donor-atom repulsion energy

considerations predict small bite angles for trigonal prismatic complexes,[3] and indeed the average bite angle for the acetylacetonate ligands (81.81°) is among the lowest found for 2,4-pentanedionate coordinated to manganese(II).[23] The only other case found in literature where the 2,4-pentanedionato ligand coordinated to Mn(II) has a bite angle smaller than 82°, is in the structure $[Mn^{II}(Mn^{II}(acac)_3)_2]$, in which the two peripheral Mn(II) ions also have a trigonal prismatic coordination geometry.[24]

6.3.2 Trigonal prism vs octahedron

Why does $[Mn(acac)_2(bpy)]$ adopt a trigonal prismatic coordination geometry in the solid phase, and why does the complex $[Mn(acac)_2(phen)]$ not do so? The electronic structures for $[Mn(acac)_2(bpy)]$ and $[Mn(acac)_2(phen)]$ are very nearly identical. Electronic effects will not play a major role in determining their preference for either the prism or the octahedron, however. The high-spin d^5 Mn(II) ion has no ligand field stabilization and no large degree of π-bonding is present, since the magnetic data shows both complexes having a spin state of S = 5/2. This value would be lower if π-bonding would take place to the extent of that found in for example rhenium dithiolene complexes.[25] In solution both complexes have a similar structure, as can be judged from their EPR spectra in frozen solution, which are nearly identical. Their structure in solution may well be in-between the trigonal prismatic and octahedral geometry, due to dynamic trigonal twisting of the complexes.

The DFT calculations in vacuum show a slight (1.5 kcal/mol) preference for the octahedral geometry for $[Mn(acac)_2(phen)]$, although this "octahedral" geometry is significantly trigonally distorted. The complex $[Mn(acac)_2(bpy)]$ does not show a preference for either prism or octahedron, but there is some barrier for going from one to the other, since it does not adopt the trigonal prismatic geometry when starting from the octahedral geometry. The calculated octahedral complexes for both bpy and phen show a significant trigonal distortion of 37° (the average torsion angle between the centroids of the faces N1-O1-O3 and O2-N2-O4, see Table 6.1). This is even more than that for the starting configuration (the X-ray geometry of $[Mn(acac)_2(phen)]$, see Figure 6.8) which

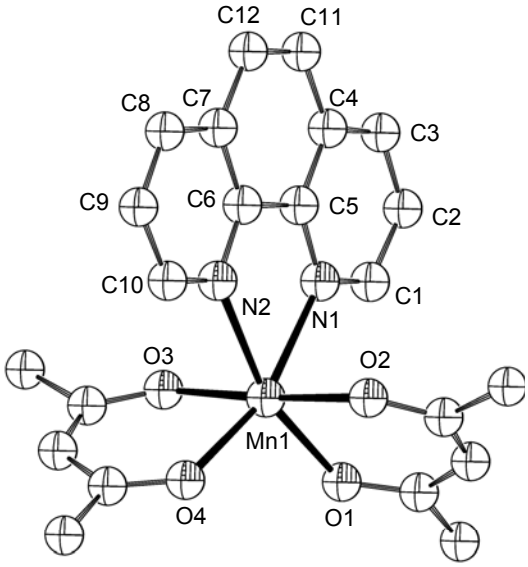

Figure 6.8: Molecular structure of $[Mn(acac)_2(phen)]$. Hydrogen atoms are omitted for clarity. The X-ray coordinates were taken from the cambridge structural database (code PEACMN). The atoms were relabeled to match the labeling of the atoms in $[Mn(acac)_2(bpy)]$.

has a trigonal distortion of 41.37° (for a regular octahedron this angle is 60°). Apparently, for both complexes a driving force towards the trigonal-prismatic geometry is present. The calculations also show that the prismatic geometry is only stable for the high-spin complexes, the complex [Mn(acac)$_2$(bpy)] spontaneously adopts an octahedral geometry when the calculation is performed with S=1/2. This behavior is to be expected, since for the low-spin Mn(II) ion ligand field stabilisation energy does play a role and the octahedral geometry is now significantly lower in energy compared to the trigonal prismatic conformation.[15]

Contrary to expectation, the difference in rigidity between the bpy and phen ligand does not seem to have a large influence on the coordination geometry. Comparing the torsion angles for the calculated prismatic complexes in Table 6.2, it can be seen that the phen ligand can be regarded as more rigid than the bpy ligand, judging by the torsion angle N1-C5-C6-N2, which is 0.61° for phen vs 4.42° for bpy. The same values are found for the calculated octahedral complexes. The deviation from a perfect prism is slightly larger for the phen complex, however, whereas for the calculated octahedral complexes the average trigonal distortion is identical. Furthermore, in the crystal structures the bpy and phen N1-C5-C6-N2 torsion angles are nearly identical, yet the coordination geometry is certainly different.

It thus seems that an important factor for determining the preference for octahedral vs trigonal prismatic geometry for the complexes [Mn(acac)$_2$(bpy)] and [Mn(acac)$_2$(phen)] is the crystal structure packing. The phen ligand is slightly more bulky than bpy and this could prevent the formation of a crystal lattice that is packed in such a way as to stabilize the trigonal prismatic geometry.

6.4 Conclusion

The trigonal-prismatic and octahedral environments in the compounds [Mn(acac)$_2$(bpy)] and [Mn(acac)$_2$(phen)] are both stable and very similar in energy for the high spin state. However, in the solid state [Mn(acac)$_2$(phen)] favours a (distorted) octahedral geometry whereas [Mn(acac)$_2$(bpy)] adopts a nearly perfect trigonal prismatic geometry. Since the rigidity of the dinitrogen ligand does not seem to play a role and the energy difference between different ligand environments for the complexes in the vacuum is quite small, packing effects in the crystal lattice must play an important role in determining the final solid-state structure.

6.5 Experimental Section

6.5.1 Materials

2,2'-bipyridine (bpy) and acetylacetone (Hacac) were purchased from Acros and used as received. [Mn(II)(acac)$_2$(H$_2$O)$_2$] was prepared according to a literature procedure.[26] Methanol was distilled from CaH$_2$ and stored on 3 Å molecular sieves under an argon atmosphere prior to use.

6.5.2 Synthesis of [Mn(acac)$_2$(bpy)]

The title compound was synthesized using a slightly modified procedure from that published in literature.[21] The reaction was performed in an argon atmosphere using standard Schlenk techniques. To a stirring, dark orange solution of [Mn(acac)$_2$(H$_2$O)$_2$] (1 g, 3.46 mmol) in 20 ml of methanol was added a solution of bpy (1.08 g, 6.92 mmol) in 10 ml of methanol. After 1 minute of stirring, [Mn(acac)$_2$(bpy)] precipitated as a bright yellow micro-crystalline material. Stirring was continued for an additional 15 minutes and then the product was filtered under argon and dried for 24 hours at room temperature under reduced pressure. Yield: 0.95 g (67%). Anal. Calc. for $C_{20}H_{22}N_2O_4Mn$: C 58.68; H 5.42; N 6.84. Found: C 58.51; H 5.26; N 7.08.

The filtrate was stored overnight at –20 °C. Yellow, prismatic-shaped single crystals precipitated. One of these crystals was used to determine the crystal structure.

6.5.3 Physical measurements

Elemental analyses on C, H and N was performed on a Perkin Elmer series II CHNS/O Analyzer 2400. The IR spectrum was recorded on a Perkin-Elmer FT-IR Paragon 1000 spectrophotometer, using a CsI pellet (4000–200 cm^{-1}, resolution 1 cm^{-1}). Ligand field spectra were obtained on a Perkin-Elmer Lambda 900 spectrophotometer. The diffuse-reflectance technique was used with MgO as a reference for the solid compound. Electron paramagnetic resonance measurements were performed using a JEOL JES-RE2X ESR Spectrometer with a JEOL X-band microwave, a JEOL electromagnet and a JEOL ESPRIT 330 ESR Datasystem unit. A special quartz Dewar flask was used for measurements at liquid nitrogen temperature (77 K). Magnetic susceptibility measurements (5-300 K) were carried out using a Quantum Design MPMS-5 5T SQUID magnetometer (measurements carried out at 1000 Gauss). Data were corrected for magnetization of the sample holder and for diamagnetic contributions, which were estimated from the Pascal constants.

6.5.4 DFT calculations

Density functional theory (DFT) calculations were performed to address the question of the preference for a specific coordination geometry in the Mn(II) complex [Mn(acac)$_2$(bpy)]. The relative energy of the trigonal prismatic versus the octahedral coordination geometry was calculated for the complex [Mn(acac)$_2$(bpy)] in the vacuum. For comparison the same relative energy difference was calculated for the related phenantroline compound [Mn(acac)$_2$(phen)], which is known to have a distorted octahedral environment about the Mn atom in the solid state.[22]

The hybrid B3LYP exchange and correlation functional was used.[27] All self-consistent field (SCF) calculations were done using the 6-31G(d,p) gaussian basis set and were performed with the Gaussian 98 package.[28] The geometries of the various complexes were fully optimised without imposing any symmetry constraint. All calculations were spin unrestricted and the relative stability of the different spin states were checked

6.5.5 X-ray crystallographic study

A crystal of dimensions 0.10 × 0.15 × 0.35 mm was selected from a batch of yellow prisms, obtained from the filtrate of the reaction mixture overnight at –20 °C. Crystal data and details on data collection are listed in Table 6.3.

Table 6.3 Crystallographic data for $[Mn(acac)_2(bpy)]$

Formula	$C_{20}H_{22}N_2O_4Mn$
M.W.	409.34
Crystal system	Hexagonal
Space group	$P6_1$
a (Å)	8.0482(9)
c (Å)	51.602(10)
V (Å^3)	2894.6(7)
Z	6
λ (Mo Kα)	0.71073
T (K)	150
ρ_{calc} (g cm^{-3})	1.4089(3)
μ (mm^{-1})	0.712
R [I > 2σ(I)][a]	0.0291
w$R2$[b]	0.0584
GoF	1.035

[a] $R = \Sigma(||F_o|-|F_c||)/\Sigma|F_o|$

[b] $wR2 = \{\Sigma[w(F_o^2-F_c^2)^2]/\Sigma[w(F_o^2)^2]\}^{1/2}$

Data were collected on an Enraf-Nonius KappaCCD area detector on a rotating anode. 30196 Reflections were measured (1.0° < θ < 25.37°), 3375 of which were independent (R_{int} = 0.0528). The structure was solved by Patterson methods using DIRDIF[29] and refined on F^2 using SHELXL-97-2.[30] Hydrogen atoms were included in the refinement on calculated positions, riding on their carrier atoms. Methyl hydrogen atoms were refined as a rigid group, allowing for rotation around the C-C bond. Non-hydrogen atoms were refined with anisotropic displacement parameters Hydrogen atoms were refined with a fixed isotropic displacement parameter linked to the value of the equivalent isotropic displacement parameter of their carrier atoms. A total of 248 parameters were refined. All peaks in the final difference Fourier map were in the range -0.19 < Δρ < 0.18 e Å^{-3}. The Flack *x*-parameter,[31] derived during the final structure-factor calculation, amounts to -0.012(14), indicating a correctly assigned absolute structure. Refinement of the inverse absolute structure resulted in an *x*-parameter of 0.97(2) (value derived during the final structure-factor calculation). Figures of merit for this inverted structure are $R1$ = 0.0428, w$R2$ = 0.1067 and S = 1.040

References

[1] R. Eisenberg, J. A. Ibers, *J. Am. Chem. Soc.* **1965**, *87*, 3777.

[2] C. L. Beswick, J. M. Schullman, E. I. Stiefel, in *Dithiolene Chemistry: Synthesis, Properties and Applications, Vol. 52* (Ed.: E. I. Stiefel), John Wiley & sons, inc., Hoboken, New Jersey, **2004**, pp. 55.

[3] D. L. Kepert, in *Comprehensive Coordination Chemistry, Vol. 1* (Ed.: G. Wilkinson), Pergamon, Oxford, **1987**, p. 61.

[4] M. F. Lappert, C. L. Raston, B. W. Skelton, A. H. White, *J. Chem. Soc. Chem. Comm.* **1981**, 485.
[5] R. E. Moriarty, R. Bau, R. D. Ernst, *J. Chem. Soc. Chem. Comm.* **1972**, 1242.
[6] P. S. Skell, M. J. McGlinchey, *Angew. Chem. Int. Edit.* **1975**, *14*, 195.
[7] A. S. Attia, C. G. Pierpont, *Inorg. Chem.* **1995**, *34*, 1172.
[8] C. L. Simpson, C. G. Pierpont, *Inorg. Chem.* **1992**, *31*, 4308.
[9] O. S. Jung, C. G. Pierpont, *Inorg. Chem.* **1994**, *33*, 2227.
[10] M. L. Kirk, R. L. McNaughton, M. E. Helton, in *Dithiolene Chemistry: Synthesis, Properties and Applications, Vol. 52* (Ed.: E. I. Stiefel), John Wiley & sons, inc., Hoboken, New Jersey, **2004**, pp. 111.
[11] J. L. Martin, J. Takats, *Can. J. Chem.* **1989**, *67*, 1914.
[12] P. M. Morse, G. S. Girolami, *J. Am. Chem. Soc.* **1989**, *111*, 4114.
[13] J. C. Friese, A. Krol, C. Puke, K. Kirschbaum, D. M. Giolando, *Inorg. Chem.* **2000**, *39*, 1496.
[14] S. G. Sreerama, S. Pal, *Inorg. Chem. Commun.* **2001**, *4*, 656.
[15] R. a. d. Wentwort, *Coord Chem Rev* **1972**, *9*, 171.
[16] E. Larsen, G. N. Lamar, B. E. Wagner, R. H. Holm, J. E. Parks, *Inorg. Chem.* **1972**, *11*, 2652.
[17] R. van Gorkum, E. Bouwman, J. Reedijk, *Inorg. Chem.* **2004**, *43*, 2456.
[18] G. C. Percy, D. A. Thornton, *J. Mol. Struct.* **1971**, *10*, 39.
[19] K. Kaeriyama, *Bull. Chem. Soc. Japan* **1974**, *47*, 753.
[20] O. Kahn, *Molecular Magnetism*, Wiley-VCH Inc., New York, **1993**, pp. 14.
[21] F. P. Dwyer, A. M. Sargeson, *J. Proc. Roy. Soc. NSW* **1956**, *90*, 29.
[22] F. S. Stephens, *Acta Crystallogr. Sect. B* **1977**, *33*, 3492.
[23] F. H. Allen, *Acta Crystallogr. Sect. B* **2002**, *58*, 380.
[24] S. Shibata, S. Onuma, H. Inoue, *Inorg. Chem.* **1985**, *24*, 1723.
[25] E. I. Stiefel, Eisenber.R, Rosenber.Rc, H. B. Gray, *J. Am. Chem. Soc.* **1966**, *88*, 2956.
[26] R. G. Charles, in *Inorg. Synth., Vol. VI* (Ed.: E. G. Rochow), McGraw-Hill, London, **1960**, pp. 164.
[27] P. J. Stephens, F. J. Devlin, C. F. Chabalowski, M. J. Frisch, *J. Phys. Chem.* **1994**, *98*, 11623.
[28] M. J. Frisch, G. W. Trucks, H. B. Schlegel, G. E. Scuseria, M. A. Robb, J. R. Cheeseman, V. G. Zakrzewski, J. A. M. Jr., R. E. Stratmann, J. C. Burant, S. Dapprich, J. M. Millam, A. D. Daniels, K. N. Kudin, M. C. Strain, Ö. Farkas, J. Tomasi, V. Barone, M. Cossi, R. Cammi, B. Mennucci, C. Pomelli, C. Adamo, S. Clifford, J. Ochterski, G. A. Petersson, P. Y. Ayala, Q. Cui, K. Morokuma, P. Salvador, J. J. Dannenberg, D. K. Malick, A. D. Rabuck, K. Raghavachari, J. B. Foresman, J. Cioslowski, J. V. Ortiz, A. G. Baboul, B. B. Stefanov, G. Liu, A. Liashenko, P. Piskorz, I. Komáromi, R. Gomperts, R. L. Martin, D. J. Fox, T. Keith, M. A. Al-Laham, C. Y. Peng, A. Nanayakkara, M. Challacombe, P. M. W. Gill, B. Johnson, W. Chen, M. W. Wong, J. L. Andres, C. Gonzalez, M. Head-Gordon, E. S. Replogle, J. A. Pople; *Gaussian 98*, Gaussian, Inc., Pittsburgh, PA, **1998**.
[29] P. T. Beurskens, G. Admiraal, G. Beurskens, W. P. Bosman, S. García-Granda, R. O. Gould, J. M. M. Smits, C. Smykalla: The DIRDIF99 program system;, University of Nijmegen, The Netherlands, **1999**.
[30] G. M. Sheldrick; SHELXL-97-2, University of Götingen, Germany, **1997**.
[31] H. D. Flack, *Acta Crystallogr. Sect. A* **1983**, *39*, 876.